Stopping power of hafnium by proton impact and the importance of relativistic $4f$ electrons

C. C. Montanari,* A. M. P. Mendez, D. M. Mitnik, and J. E. Miraglia

Instituto de Astronomía y Física del Espacio, Consejo Nacional de Investigaciones Científicas y Técnicas - Universidad de Buenos Aires, Pabellón IAFE, 1428 Buenos Aires, Argentina

P.A. Miranda, R. Correa, J. Wachter, and M. Aguilera

Departamento de Física, Facultad de Ciencias Naturales, Matemática y del Medio Ambiente. Universidad Tecnológica Metropolitana. 7800002, Chile

E. Alves

Centro de Ciências e Tecnologias Nucleares, Instituto Superior Técnico, Universidade de Lisboa, 2696-953 Sacavém, Portugal and Instituto de Plasma e Fusão Nuclear, Instituto Superior Técnico, Universidade de Lisboa, 2696-953 Sacavém, Portugal

N. Catarino and R.C. da Silva

Centro de Ciências e Tecnologias Nucleares, Instituto Superior Técnico, Universidade de Lisboa, 2696-953 Sacavém, Portugal

(Dated: April 3, 2020)

The stopping power of protons through Hf foil has been studied both experimentally and theoretically. The measurements were performed at the Laboratory of Accelerators and X-Ray Diffraction in Lisbon, by using the transmission method on self-supporting stopping material. The overall uncertainty of around 5% was established over the protons energy range (0.6-2.5) MeV. The theoretical developments involved fully relativistic atomic structure calculations for Hf, which required the solution of the Dirac equation. The shell-wise local plasma approximation (SLPA) was used to describe the energy transferred to the bound $1s$-$4f$ electrons, and the outer four electrons were considered as a free electron gas (FEG). We found the relativistic description of the $4f$-shell and the screening between $4f$ and $5p$ electrons are decisive around the stopping maximum. Present theoretical and experimental results are in very good agreement in the energy region of the new measurements. However, the present theoretical stopping cross sections show substantial differences with the most used semi-empirical models (SRIM2013 and ICRU-49) at intermediate to low energies. Our calculations suggest the stopping maximum higher and shifted to lower energies than these previous predictions. Future measurements below 100 keV would be decisive for a better knowledge around the maximum and below.

PACS numbers: 34.50.Bw

Keywords: Stopping power, hafnium, Relativistic atomic structure, Transmission method

I. INTRODUCTION

For impact energies above a few keV/amu, monoenergetic charged particles penetrating a foil of any material lose their energy through a series of consecutive inelastic collisions, mainly with target electrons [1, 2]. The information given by the energy loss process is essential not only to have a better knowledge of the physics behind the fundamental interactions, but also because it plays an important role in many applied fields such as materials science, nuclear physics, ionic implantation and radiotherapy [2, 3]. Experimental data on ion mean energy loss per unit path $S(E)$ is of crucial relevance to check the reliability of semi-empirical models and to determine some key parameters [4–6]. The experimental data available is often rather scarce, which is troublesome when the material under study corresponds to an element of low occurrence on the Earth's upper crust, such as hafnium.

So far, only one experimental work has been published regarding the stopping power cross section of pure hafnium for protons [7], while more attention has been recently given to studies involving hafnium oxide due to its practical use [8–11]. It is well known that significant attention has been paid in recent years to transition metal-oxides such as HfO_2 because of their potential as alternative gate dielectrics to replace SiO_2 for the future generation of nano-electronics with less than 45 nm gate length [12, 13]. Some important physical properties of the above mentioned metal-oxide films depend on its thickness, which is often measured by using Rutherford Backscattering Spectrometry [14, 15], a method that relies heavily on the determination of the stopping power of ion beams in the material of interest.

In this study, we report experimental stopping power cross sections over the incident energy range (0.6-2.5)

* mclaudia@iafe.uba.ar

MeV for protons crossing self-supported Hf thin-film by using the transmission method. We aim not only to upgrade stopping power data compilations [16, 17] but also to provide useful information about the processes governing the slowing down of protons in multi-electronic targets. In the rare earth metals, the $4f$ electrons play a relevant role in the stopping power, being the first shell of bound electrons below the conduction band. As already noted [18], the free electron gas (FEG) shows unexpected behavior in these elements, which casts doubts on its proper description. In the case of Hf, we found the contribution of the $4f$-shell decisive even at impact energies around the stopping maximum, as shown later.

The theoretical approach implemented in this work uses the shell-wise local plasma approximation (SLPA) [19] to describe the energy transferred to the bound $1s$-$4f$ electrons, and two different models for the FEG: the screened potential with cusp condition model (SPCC) [20], which is non-linear binary formalism; and the Mermin-Lindhard dielectric formalism (ML) [21], for energies around the stopping maximum and above. Our model requires the relativistic wave functions and binding energies of Hf, and considers 4 electrons per atom in the FEG [22]. Hf has the extra interest of the filled $4f$-subshell (with 14 electrons) as the main contribution below the FEG, causing the stopping cross sections to be very sensitive to a good description of this shell. The screening among the $4f$ and $5p$ electrons has been considered and found to play a major role within the SLPA calculations.

The experimental details and data are given in Section II, while the theoretical method is explained in Section III. Present theoretical and experimental values are finally compared to the available experimental values [7], the ICRU-49 calculations [23] and the SRIM-2013 package [24]. Conclusions and discussions are given in Section V. All the present data can be found at the Zenodo platform [25].

II. EXPERIMENTAL ARRANGEMENTS

A. Accelerator and scattering Chamber

The procedure used in this work to obtain stopping power data is essentially the same as described in Ref. [26]. The present measurements were made at the IST/LATR (Laboratory of Accelerators and X-Ray Diffraction) in Lisbon. This facility uses a 2.5 MV Van de Graaff accelerator to deliver $^1H^+$ primary ion beams through a series of electrostatic lenses and collimators onto a thin Au/SiO_2 sample which is used as a scattering center. This sample was placed in the center of a RBS/C scattering chamber, where a high vacuum (pressure of $\sim 10^{-6}$ Torr) was maintained during the measurements. The beam current on the sample was kept at around 5.0 nA to attain sufficient statistics in each particle spectrum. By using a beam spot of about 1.0 mm in diameter, a solid angle of 11.4 msr was attained. The overall energy resolution (FWHM) of the detection system was about 15 keV relative to 5.486 MeV alpha particles from a ^{241}Am source.

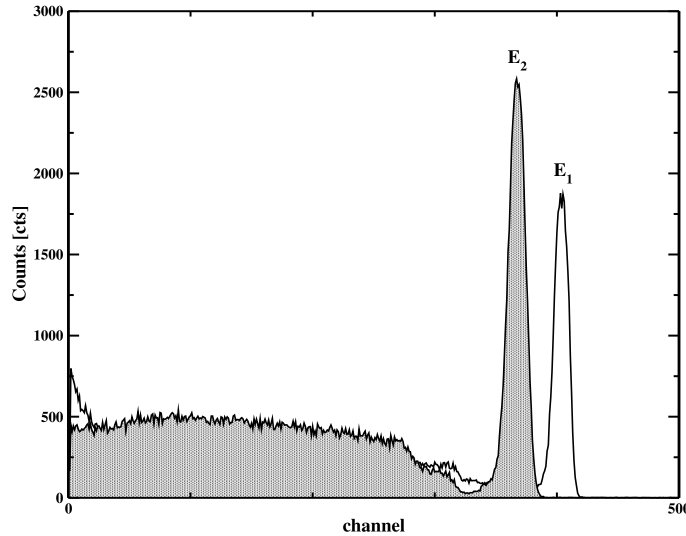

FIG. 1. RBS spectrum for $E_{\rm avg} = 921.1$ keV protons on hafnium sample which is subsequently used to determine the energy loss in the foil.

B. Target

The stopping material under analysis was a hafnium foil with nominal thickness of 1.0 μm and 99.95% purity which was supplied by Lebow Company [27]. However, a more precise thickness value was achieved by measuring the energy loss of alpha particles coming from a calibrated (^{239}Pu, ^{241}Am, ^{244}Cm) source. From the alpha spectra with and without the Hf foil interposed, the characteristic energy shift δE was measured and then combined with the stopping power for 5.486 MeV alphas on hafnium (55.69 eV/10^{15} at/cm^2) found in Ref. [24] to obtain an areal density of $(4.13 \pm 0.21) \times 10^{19}$ at/cm^2 which corresponds to a thickness of $0.920 \pm 0.046 \mu$m.

C. Energy loss measurement

Once the beam impinges on the Au/SiO_2 sample, protons are back-scattered towards a Si surface barrier detector located at 140° relative to the initial beam direction. Fig. 1 shows two particle spectra where ion energies E_2 and E_1 are associated to a placed and removed hafnium sample, respectively. Both energy distributions were fitted by Gaussian functions to obtain the mean energy and width (FWHM) of the peaks [28], and from the difference between these two peak positions in the spectrum, the total energy loss $\Delta E = (E_1 - E_2)$ in the foil was calculated. As established in previous studies [5, 26], the experimental stopping power cross sections $\varepsilon(E)$ are determined at some mean energy E_{avg} by measuring the ion energy losses ΔE within the investigated Hf foil, which has a mean thickness denoted by Δx. In this way, only when the energy loss fraction $\Delta E/E_{\text{avg}}$ across the Hf foil is not exceeding 20% it is possible to define the stopping cross section by [29, 30]:

$$\varepsilon(E) = \frac{S(E)}{N} = -\frac{dE}{N\,dx} \approx -\frac{\Delta E}{N\Delta x}, \tag{1}$$

where N denotes the atomic number density (atoms cm^{-3}) of the material under study. When this condition was not fulfilled, a small correction to the mean energies E_{avg} was applied in order to account for the nonlinear dependence on ion energy of stopping powers [31, 32].

III. THEORETICAL METHOD

The energy loss of ions in metal targets responds to different physical mechanisms, depending on the impact ion velocity. At low velocities, the binary collisions are responsible for the loss of energy by the ion. The main contribution is the ionization of electrons of the metal conduction band, which is well approximated by a free electron gas (FEG) of Fermi velocity v_F. Above certain velocity (i.e. $v \geq 1.5\,v_F$), not only binary but also collective excitations (plasmons) occur [20]. Moreover, at high energies, also the bound electrons contribute to the stopping power. The method used in this work combines a description for the interaction with the valence (or conduction) electrons as a FEG, and a different one for the interaction with the bound electrons.

We used the SPCC model [20] to describe the stopping power of low velocity charged particles in the FEG. It is a non-perturbative binary collisional approximation, thus valid at energies below that of plasmon excitations. The SPCC [20] is based on a screened central potential with cusp condition of the electronic density close to the projectile. This model proved to give a good description of the induced electron density even for negative projectiles [20], and reproduces the low velocity proton-antiproton differences in the stopping power (Barkas effect). The SPCC formalism only depends on the Wigner-Seitz radio, r_S, which is a measure of the electronic density of the FEG. For metals of well-known r_S, the SPCC describes correctly the low energy experimental stopping data [20], agreeing with the DFT results by Echenique and coworkers [33, 34] at $v = 0$.

Hafnium ($Z = 72$, [Xe] $4f^{14}\,6s^2\,5d^1_{3/2}\,5d^1_{5/2}$), belongs to the first groups of transition metals, with four electrons as FEG (theoretical $r_S = 2.14$ a.u.) and $1s$-$4f$ electrons bound. We compared the computed r_S with the experimental value obtained from measured energy loss function by Lynch *et al* [35]. The experimental plasmon energy of Hf is $\hbar\omega_P \approx 15.8$ eV, with a width at half maximum $\delta \approx 4.4$ eV, and $r_S \approx 2.07$ a.u. [35]. The difference of less than 5% between theoretical and experimental r_S assess Hf as a canonical target [20].

Above certain impact velocity, the plasmon contribution is important (i.e. around and above the stopping maximum). An interesting value for our analysis is the minimum impact velocity to excite plasmons, v_P. In the dielectric formalism, this value can be obtained as $v_P \approx v_F[1 + (3\pi\,v_F)^{-1/2}]$ [36]. To describe the energy loss considering collective and binary excitation, we resort to the ML dielectric formalism [21], which is a linear response, perturbative approximation, so it depends on the square of the ion charge. In this formalism, the response of target electrons to the ion passage is described through the quantum dielectric function, depending on the characteristic r_S and δ parameters of the FEG.

For the stopping power due to bound electrons, the SLPA [19, 20] is employed. It is worth mentioning that the only inputs for the SLPA are the space-dependent densities of each shell in the ground state, and their binding energies. Collective processes and screening among electrons are included. Since hafnium is a relativistic target, the wave functions and binding energies must be obtained by solving the many-electron Dirac Hamiltonian. Details of these calculations have been published in [22], while Slater-type orbital expansions are given in [37]. To assess the importance of the description of bound electrons, Fig. 2 shows (a) non-relativistic [38] and our relativistic binding energies $E_{nl\pm}$, with $\pm = j \pm 1/2$; and (b) the relative errors with respect to the experimental data on solid Hf [39] from $1s$ to $4f_{\pm}$. One would expect the relativistic contributions to only affect significantly the inner shells. The relativistic binding energies of the electrons belonging to these shells are 2.5% from the experimental values, while the non-relativistic ones are within $\sim$10%. Moreover, we notice the relativistic corrections greatly influences the outer $5p$ and $4f$ shells. This effect may be a consequence of the orthogonality with the relativistic inner shells. Also, the sign of the binding energy deviations is inverted near the FEG limit, i.e. the electrons go from being more bounded –than the experimental values– to being less bounded. This change of sign can be attributed to the fact that the experimental values correspond to hafnium in solid-state, while our theoretical calculations correspond to the element in the gas phase.

Our relativistic binding energies present spin-orbit split. However, in total stopping power, where the initial state of the excited electron is not measured, the quantum uncertainty in energy ΔE melts this split. The criteria $\Delta E \Delta t \geq \hbar/2$ merges the energies $E_{nl+} - E_{nl-}$ for sufficiently small values of Δt (the collisional mean-time). In fact, at sufficiently high impact velocity, we can expect all target electrons to respond together to the ion passage [40, 41]. Following previous work [42], the collisional time is estimated as $\Delta t \approx \langle r_i \rangle / v$, with $\langle r_i \rangle$ and v being the orbital mean radio and impact velocity, respectively.

The SLPA calculates the contribution of each subshell

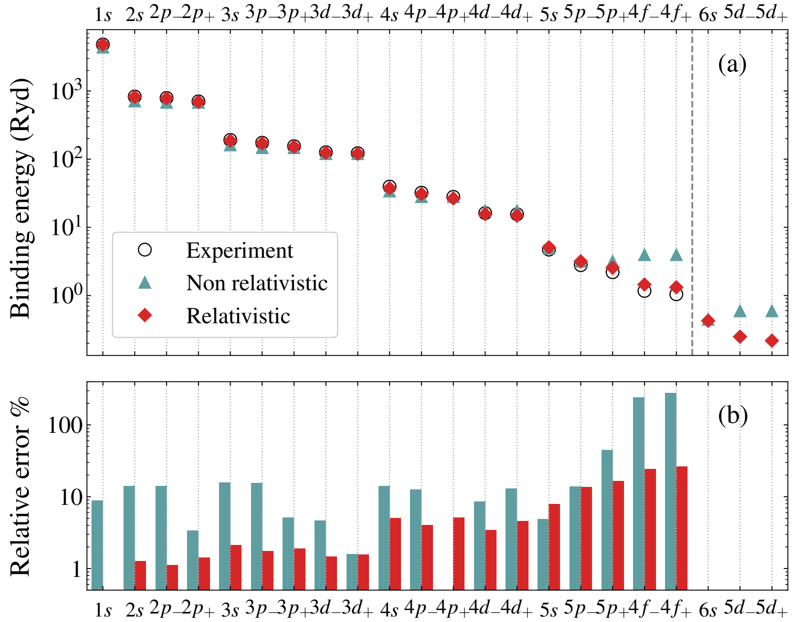

FIG. 2. (a) Binding energies of Hf. Non-relativistic and relativistic calculations are given with filled symbols. Experimental measurements for solids [39] are depicted with open circles. (b) Corresponding relative errors respect to experimental data.

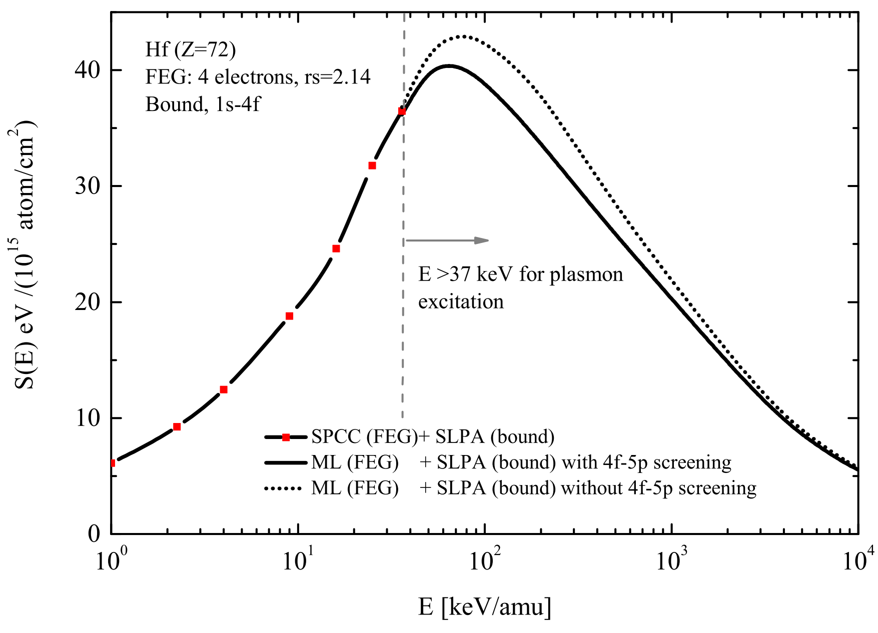

FIG. 3. Theoretical total stopping cross sections of protons in hafnium adding FEG and bound $1s$-$4f$ contributions, as mentioned in the inset. The vertical grey dashed-line indicates the energy above which plasmon excitation is possible. The SLPA total stopping values for $1s$-$4f$ bound electrons with and without $5p$-$4f$ screening are displayed with solid and dotted lines, respectively.

of bound electrons to the total stopping cross sections. We found that for every sub-shell of Hf, at the impact energy at which this sub-shell began to contribute, the spin-orbit split was unresolved. Then, the nl-electrons should be considered together, responding to the ion passage as a single gas of electrons with density $\delta_{nl}(r)$ and a mean binding energy E_{nl}. This feature is important within the SLPA calculations because it accounts for the screening among electrons of the *same* binding energy. For example, the $4f_-$ and $4f_+$ of Hf can only be resolved for impact energies $E < 0.05$ keV, but the contribution of $4f$ to the total stopping is negligible for $E < 40$ keV. Moreover, the $5p$ and $4f$ electrons of Hf are very close in energy ($\Delta E_{5p-4f} \approx 1$ a.u. [22]) and they react together for impact energies $E > 40$ keV (inter-shell screening).

In Fig. 3, we display the present theoretical stopping cross section of Hf for protons with and without the $5p$-$4f$ screening. We added the FEG and the bound electron contributions as explained above. The minimum energy for plasmon excitation was estimated to 37 keV. We used the non-perturbative SPCC model for impact energies $E \leq 37$ keV, and the perturbative ML calculation above this energy. Clearly, considering $5p$-$4f$ electrons as a single group of 20 electrons with screening among them gives lower stopping values than the addition of the separate $5p$ and $4f$ contributions. Notice that this shell correction can only be considered within a many electron model such as the SLPA.

IV. ANALYSIS OF THE RESULTS AND DISCUSSION

The present data and theoretical results are displayed in Table I, and Fig. 4. As can be seen in Table I, an overall relative uncertainty of around 5% was achieved for the experimental stopping power values, which are mainly due to the uncertainty in the hafnium foil thickness.

In Fig. 4, we have good agreement between the present theoretical results and the measurements displayed in Table I. Our theoretical approach also agrees with previous data by Sirotinin [7], except for the lowest energy measurement at 80 keV. It is interesting that our full theoretical curve differs from SRIM-2013 for impact energies below 100 keV. We obtain a stopping maximum around 40×10^{-15} eV cm^2/atom at 65 keV. Instead, following the up-to-now only set of data [7], SRIM-2013 suggests a lower stopping maximum at impact energy of 115 kev. It is worth mentioning that similar theoretical results using the experimental $r_S = 2.07$ a.u. instead of the theoretical $r_S = 2.14$ a.u. give the stopping maximum at the same impact energy but 4% higher. Future experiments for impact energies below 100 keV would be important to complete this study.

V. CONCLUSION

In this work, we have used the transmission method to experimentally determine stopping power cross section values for (0.6-2.5) MeV protons incident on self-supporting Hf foils with an overall uncertainty of around 5%. Additionally, we calculated values extracted from the theoretical framework that involved the relativistic wave functions and binding energies of Hf, and considered four electrons per atom in the free electron gas. The shell-wise local plasma approximation was employed to describe the energy transferred to the bound $1s$-$4f$ electrons, and two different models for the FEG: the screened potential with cusp condition (SPCC model) for energies below that of the plasmon excitation, and the Mermin-Lindhard dielectric formalism, for energies around the stopping maximum and above. Present theoretical stopping cross sections cover an extensive energy range from 1 keV/amu-10 meV/amu.

At high impact energies, the new stopping measurements are in good agreement with our theoretical results, with previous experimental data and semi-empirical values by SRIM-2013 and ICRU-49. However, we call the attention that around the stopping maximum and at lower impact energies the difference between our full-theoretical results and SRIM is substantial. To the best of our knowledge, these are the first theoretical calculations of stopping in Hf taking into account the atomic relativistic effect. Future experiments for impact energies below 100 keV would be important to complete this study.

ACKNOWLEDGMENTS

This work was funded by VRAC Grant Number L1-17 of Universidad Tecnológica Metropolitana, Chile; also by the Consejo Nacional de Investigaciones Científicas y Técnicas (CONICET), the Agencia Nacional de Promoción Científica y Tecnológica (ANPCyT), and Universidad de Buenos Aires (UBA), from Argentina.

The authors gratefully acknowledge the invaluable contribution of F. Baptista from ITN/IST-UTL, Sacavém, Portugal for his constant availability.

[1] W.K. Chu, J.W. Mayer, and M.A. Nicolet, *Backscattering Spectrometry* (Academic Press, New York, 1978).

[2] P. Sigmund, *Particle Penetration and Radiation Effects. General Aspects and Stopping of Swift Point Charges.* (Springer Series in Solid-State Sciences, Springer, Berlin, 2006), Vol. 151.

[3] D. Schardt, T. Elsässer, D. Schulz-Ertner, Rev. Mod. Phys. **82**, 383-425 (2010).

[4] P.K. Diwan, S. Kumar, Nucl. Instr. and Meth. B **359**, 78-84 (2015).

[5] D. Moussa, S. Damache and S. Ouichaoui, Nucl. Instr. and Meth. B **268**, 1754-1758 (2010); **343**, 44-47 (2015).

[6] S. Damache, S. Ouichaoui, A. Belhout, A. Medouni and I. Toumert, Nucl. Instr. and Meth. B **225**, 449-463 (2004).

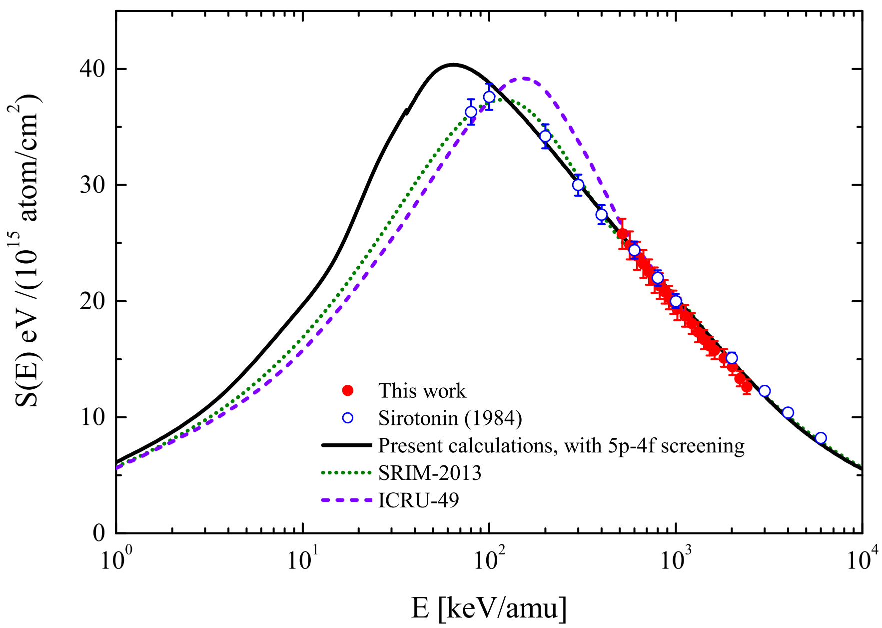

FIG. 4. Stopping power cross section of hafnium for protons. Symbols: solid circles, present values; open circles, previous data [7]. Curves: Black solid-line, present full theoretical results with $4f$-$5p$ screening; violet dashed-line, values from ICRU-49 [23], and green dotted line, SRIM-2013 [24].

TABLE I. Stopping power values S_{exp} of hafnium for protons measured in this work. $\Delta E/E$ values are also shown.

E_{avg} keV	S_{exp} eV/(10^{15} at/cm^2)	$\Delta E/E$ %	E_{avg} keV	S_{exp} eV/(10^{15} at/cm^2)	$\Delta E/E$ %	E_{avg} keV	S_{exp} eV/(10^{15} at/cm^2)	$\Delta E/E$ %
516.6	25.8 ± 1.3	20.5	1170.3	18.25 ± 0.91	6.4	1813.4	15.10 ± 0.76	3.4
567.8	24.8 ± 1.2	17.9	1220.0	18.08 ± 0.90	6.1	1862.7	14.79 ± 0.74	3.3
618.8	23.9 ± 1.2	15.8	1269.6	17.57 ± 0.88	5.7	1912.0	14.21 ± 0.71	3.0
669.6	23.2 ± 1.2	14.2	1319.2	17.32 ± 0.87	5.4	1961.2	14.46 ± 0.72	3.0
720.1	22.5 ± 1.1	12.8	1368.8	17.15 ± 0.86	5.1	2010.4	14.34 ± 0.72	2.9
770.5	21.8 ± 1.1	11.6	1418.3	16.69 ± 0.83	4.8	2059.6	13.76 ± 0.69	2.7
820.8	21.3 ± 1.1	10.7	1467.8	16.43 ± 0.82	4.6	2108.8	13.78 ± 0.69	2.7
871.0	20.8 ± 1.0	9.8	1517.2	16.13 ± 0.81	4.4	2158.0	13.70 ± 0.69	2.6
921.1	20.3 ± 1.0	9.1	1566.7	16.04 ± 0.80	4.2	2206.5	13.33 ± 0.67	2.5
971.1	19.9 ± 1.0	8.4	1616.0	15.77 ± 0.79	4.0	2256.4	13.27 ± 0.66	2.4
1021.0	19.33 ± 0.97	7.8	1665.4	15.51 ± 0.78	3.8	2305.5	13.07 ± 0.65	2.3
1070.8	19.03 ± 0.95	7.3	1714.8	15.46 ± 0.77	3.7	2354.7	12.91 ± 0.65	2.2
1120.6	18.73 ± 0.94	6.9	1764.1	14.93 ± 0.75	3.5	2403.8	12.61 ± 0.63	2.2

[7] E.I. Sirotinin, A.F. Tulinov, V.A. Khodyrev, V.N. Mizgulin, Nucl. Instr. and Meth. B **4**, 337-345 (1984).

[8] I. Abril, M. Behar, R. Garcia Molina, R.C. Fadanelli, L.C.C.M. Nagamine, P.L. Grande, L. Schünemann, C.D. Denton, N.R. Arista, E.B. Saitovich, Eur. Phys. J. D 54, 65-70 (2009).

[9] M. Behar, R.C. Fadanelli, I. Abril, R. Garcia-Molina, C.D. Denton, L.C.C.M. Nagamine, N.R. Arista, Phys. Rev. A **80**, 062901 (2009).

[10] D. Primetzhofer, Nucl. Instr. and Meth. B **320**, 100-103 (2014).

[11] D. Roth, B. Bruckner, G. Undeutsch, V. Paneta, A.I. Mardare, C.L. McGahan, M. Dosmailov, J.I. Juaristi, M. Alducin, J.D. Pedarnig, R.F. Haglund, Jr., D. Primetzhofer, and P. Bauer Phys. Rev. Lett. **119**, 163401 (2017).

[12] J.H. Choi, Y. Mao, J.P. Chang, Mat. Sci. Eng. R **72**, 97-136 (2011).
[13] J. Robertson, R.M. Wallace, Mat. Sci. Eng. R **88**, 1-41 (2015).
[14] Z.B. Alfassi, *Non-destructive elemental analysis* (Blackwell Publishing, Oxford, 2001).
[15] J.R. Tesmer, M. Nastasi, J.C. Barbour, C.J. Maggiore and J.W. Mayer, *Handbook of Modern Ion Beam Material Analysis.* (Materials Research Society, Pittsburgh, 1995).
[16] https://www-nds.iaea.org/stopping/.
[17] C.C. Montanari, and P. Dimitriou, Nucl. Instr. and Meth. B **408**, 50-55 (2017).
[18] D. Roth, B. Bruckner, M. V. Moro, S. Gruber, D. Goebl, J. I. Juaristi, M. Alducin,R. Steinberger, J. Duchoslav, D. Primetzhofer, and P. Bauer, Phys. Rev. Lett. **118**, 103401 (2017).
[19] C.C. Montanari and J.E. Miraglia in *Advances in Quantum Chemistry*, edited by D. Belkić, (Elsevier, Amsterdam, 2013), Vol 65, Chap. 7, pp. 165-201.
[20] C.C. Montanari, and J.E. Miraglia, Phys. Rev. A **96**, 012707 (2017).
[21] N.D. Mermin, Phys. Rev. B **1**, 2362 (1970).
[22] A.M.P. Mendez, C.C. Montanari, D.M. Mitnik, Nucl. Instrum. Meth. B **460**, 114-118 (2019).
[23] ICRU report 49, Stopping Powers and Ranges for Protons and Alpha Particles, International Commission on Radiation Units and Measurements, 1993.
[24] J.F. Ziegler, J.P. Biersack, SRIM2013, Computer Program and Manual. Available from www.srim.org.
[25] C.C. Montanari *et al.* DOI: 10.5281/zenodo.3678785
[26] P.A. Miranda, A. Sepúlveda, J.R. Morales, T. Rodriguez, E. Burgos, H. Fernández, Nucl. Instr. and Meth. B **318**, 292-296 (2014).
[27] Lebow Company. 5960 Mandarin Ave. Goleta CA, 93117, USA.
[28] G. Sun, M. Döbelli, A.M. Müller, M. Stocker, M. Suter and L. Wacker, Nucl. Instr. and Meth. B **256**, 586-590 (2007).
[29] J. Raisanen, U. Watjen, A.J.M. Plompen, F. Munnik, Nucl. Instr. and Meth. **B** 118, 1-6 (1996).
[30] F. Schulz and J. Shchuchinzky, Nucl. Instr. and Meth. B **12**, 90-94 (1985).
[31] A.B. Chilton, J.N. Cooper and J.C. Harris, Phys. Rev. **93**, 413-418 (1954).
[32] M. Rajatora, K. Vakevainen, T. Ahlgre, E. Rauhala, J. Raisanen, K. Rakennus, Nucl. Instr. and Meth. B **119**, 457-462 (1996).
[33] P. M. Echenique, R. M. Nieminen and R. H. Ritchie, Sol. State Comm. **37**, 779-781 (1981).
[34] I. Nagy, A. Arnau, P. M. Echenique, and E. Zaremba, Phys. Rev. B **40**, 11983 (1989).
[35] D. W. Lynch, C. G. Olson, and J. H. Weaver, Phys. Rev. B **11**, 3617-3624 (1975).
[36] C. C. Montanari, J. E. Miraglia, and N. R. Arista, Phys. Rev. A **62**, 052902 (2000).
[37] A.M.P. Mendez, C.C. Montanari, D.M. Mitnik, *Slater-type orbital expansion of neutral hafnium, numerical solution of the relativistic Dirac equation*, available soon in arXiv.org.
[38] N.R. Badnell, Comput. Phys. Commun., **182**, 1528-1535 (2011).
[39] G. Williams in http://xdb.lbl.gov/Section1/Sec_1-1.html
[40] J. Lindhard, M. Scharff, Mat. Fys. Medd. Dan. Vid. Selsk **27**, 1 (1953).
[41] W. K. Chu, D. Powers, Rev. Lett. A **40**, 23 (1972).
[42] C.C. Montanari, D.M. Mitnik, C.D. Archubi, and J.E. Miraglia, Phys. Rev. A **80**, 012901 (2009).